Polymer Testing 121 (2023) 107984

Contents lists available at ScienceDirect

Polymer Testing

journal homepage: www.elsevier.com/locate/polytest

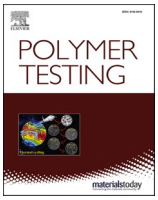

Micromechanical analysis and fracture mechanics of Poly(lactic acid) (PLA)/Polycaprolactone (PCL) binary blends

Laura Aliotta [a,b,*,1], Vito Gigante [a,b,1], Ruben Geerinck [c], Maria-Beatrice Coltelli [a,b], Andrea Lazzeri [a,b,d,**]

[a] Department of Civil and Industrial Engineering, University of Pisa, 56122, Pisa, Italy
[b] National Interuniversity Consortium of Materials Science and Technology (INSTM), 50121, Florence, Italy
[c] Centexbel, Technologiepark 70, 9052, Zwijnaarde, Belgium
[d] Planet Bioplastics s.r.l., Via San Giovanni Bosco 23, 56127, Pisa, Italy

ARTICLE INFO

Keywords:
Poly(lactic acid) (PLA)
Binary blends
Mechanical analysis
Dilatometric studies
Fracture mechanics

ABSTRACT

Even Poly(lactic acid)/polycaprolactone (PLA/PCL) blends have been studied in literature, the deformation mechanism that is related to the toughness increment with respect to pure PLA has not been investigated in detail. The novelty of this work is to understand in depth the correlation between the micromechanical deformation processes occurring in PLA/PCL blends to the macromechanical properties, their morphology and their fracture mechanism.

PLA/PCL blends containing increasing amount of PCL (from 10 up to 40 wt%) were produced. A novel characterization approach, not yet investigated for these blends, was carried out by dilatometric uniaxial tests using a videoextensometer. The shape of the dilatometric curves coupled with SEM analysis revealed how changing the PCL amount different concurrent micromechanical deformation processes occurred. When 10 wt% of PCL was added only particles debonding occurred leading to lower enhancement of elongation at break; at 20 wt% both debonding and voids growth along the tensile direction occurred, while at 40 wt% of PCL shear yielding was predominant that lead to a great enhancement of the elongation at break. The PLA/PCL blends capability to absorb energy at slow rate, was evaluated by the elasto-plastic fracture approach based on the ESIS load separation criterion. The results obtained was then correlated with the final blend morphology.

1. Introduction

Biodegradable polymers are a promising solution to reduce plastic waste especially for those applications (like packaging, non-woven tissues, textiles, etc.) where their use can decrease the environmental troubles correlated to plastic disposal [1,2]. The increment of nondegradable plastic, together with the oil depletion, has pushed up the study and the development of biodegradable plastics both from renewable and nonrenewable resources [3]. Biobased and/or biodegradable plastics are seen as potential and valid alternatives because they can redirect huge plastics amounts deriving from single-use plastic litter that commonly are difficult to recycle [4].

Among biobased and biodegradable polymers, poly(lactic acid) (PLA) is a well-known promising biobased polymer that has been used in different sectors, especially in packaging [5–8]; it possesses good mechanical properties, especially from the point of view of stiffness but, on the other hand, it is very brittle. Among the different strategies to improve the PLA toughness, summarized by Krishnan et al. [9], the most efficient method to reduce the intrinsic PLA brittleness is its physical blending with ductile polymers [10]. In literature, different biobased and/or biodegradable polymers were successfully blended with PLA such as; poly(butylene succinate) (PBS) [11–14], poly(butylene succinate-*co*-adipate) (PBSA) [15–17], poly(butylene adipate-*co*-terephthalate) (PBAT) [10,18] and poly(ε-caprolactone) (PCL) [19–21].

In this work the attention has been paid to PLA/PCL blends because they are very attractive being both PLA and PCL biodegradable and biocompatible with synergically rheological, thermal, mechanical and biodegradation properties [22–25]. PCL, currently produced from not

* Corresponding author. Department of Civil and Industrial Engineering, University of Pisa, 56122, Pisa, Italy.
** Corresponding author. National Interuniversity Consortium of Materials Science and Technology (INSTM), 50121, Florence, Italy.
E-mail addresses: laura.aliotta@unipi.it (L. Aliotta), andrea.lazzeri@unipi.it (A. Lazzeri).
[1] These authors contributed equally to the work.

https://doi.org/10.1016/j.polymertesting.2023.107984
Received 11 January 2023; Received in revised form 1 March 2023; Accepted 9 March 2023
Available online 9 March 2023

renewable sources, can be reasonably produced from renewable monomers in the future [26].

PLA/PCL are immiscible and immiscible polymer blends tend to form different phases that, depending on the extrusion compounding process parameters, can have micro or nano extension. The size of these two phases, their interfacial adhesion and their morphology affects the final mechanical properties of the blends [27]. For this reason, it is fundamental to investigate the micromechanical deformation processes that occur in physical polymeric blends; in fact, external stresses can generate numerous and different micromechanical deformation processes, generally correlated with a volume variation, that play a critical role because they are the basis of the failure of these heterogenous systems [28,29].

In this context, nevertheless different studies are present on PLA/PCL blends [20,21,30–34], they do not investigate the correlation between the micromechanical deformation processes to the macromechanical properties and fracture mechanism. In fact, when a rubber toughened material undergoes to uniaxial tensile test, the rubber particles embedded within the polymeric matrix generate voids (that, depending to the rubber particle/matrix adhesion, cavitate or debond) [29,35]; these voids will grow along the tensile direction in a second consecutive mechanism causing great differences in volume variation. Consequently, to have a clear idea of the micromechanical deformation processes, the analysis of the volume change of the polymeric blends when they undergo to uniaxial tensile test can be done thanks to the use of a video extensometer coupled with SEM analysis. This technique was applied with success in other similar PLA rubber toughened systems [10,15,29]. The use of video-controlled tensile testing equipment, developed by G'sell et al. [36,37], avoids the drawbacks correlated to the use of mechanical extensometer mainly correlated with the range limitations. Up to today this technique was adopted by G'sell et al. [37] to evaluate the deformation mechanisms of pure PLA and PCL but not of their blends. Thus, the aim of this study is to investigate how the presence of different PCL amounts (from 10 up to 40 wt%), affects the PLA micromechanical deformation process and fracture behavior (the latter investigated adopting the elasto-plastic fracture approach based on the ESIS load separation criterion [38,39]); these investigations were accompanied by melt flow index (MFI) analysis, that was found useful to study the processability features and morphology evolution associated to the injection moulding of the PLA/PCL investigated specimens.

2. Materials and methods

2.1. Materials

Poly(lactic acid) (PLA) Luminy LX175, provided by Total Corbion PLA, was used. It is a fully biobased extrusion grade PLA containing about 4% of D-lactic acid units. [mean MW: 163,000 g/mol; density: 1.24 g/cm^3 and melt flow index (MFI) (210 °C/2.16 kg) of 6 g/10 min]. Polycaprolactone (PCL), trade name Capa 6500 provided by Perstorp (Malmö, Sweden) compatible with a wide range of common thermoplastics was used. [mean MW: 50,000 g/mol; density of 1.1 g/cm^3; MFI: (190 °C/2.16 kg) of 28 g/10 min].

2.2. Blends and sample preparation

PLA/PCL binary blends containing increasing amounts of PCL (at 10, 20 and 40 wt%), were produced in pellets according to the compositions reported in Table 1. PLA and PCL were compounded in a semi-industrial Comac EBC 25HT (L/D = 44) (Comac, Cerro Maggiore, Italy) twin screw extruder. Before extrusion both polymers were dried in a Piovan DP 604–615 dryer (Piovan S.p.A., Verona, Italy). The temperature profile along the 11 extruder zones was: 150/185/185/185/185/180/180/175/170/165/165 °C. The die zone was set at 165 °C. The screw rate was 280 rpm coupled to a total mass flow rate of 15 kg/h. During the extrusion compounding the extruder head pressure decreased, passing from 24 bar for PLA to 14 bar for PLA60_PCL40.

Table 1
Blends name and composition.

Blend name	PLA (wt.%)	PCL (wt.%)
PLA	100	–
PLA90_PCL10	90	10
PLA80_PCL20	80	20
PLA60_PCL40	60	40

After their drying in the above mentioned Piovan dryer, the extruded pellets were injection moulded in a Megatech H10/18 injection moulding machine (TECNICA DUEBI s.r.l., Fabriano, Italy) to produce two specimens typology: ISO 527-1A dog bone specimens (useful dimensions: 10 mm width, 4 mm thickness and 80 mm length) and ISO 179 parallelepiped Charpy specimens (width: 10 mm, thickness: 4 mm, length: 80 mm). The main injection moulding parameters are reported in Table 2.

2.3. Melt flow rate (MFR)

The melt flow behaviour of the extruded blends granules was investigated by a Melt Flow Tester M20 (CEAST, Torino, Italy); it is an expression of melt fluidity. The MFR (melt flow rate) is defined as the weight of molten polymer passed in a defined time through a capillary of specific diameter and length (2.095 × 8 mm) by pressure applied through a weight following the ISO 1133 (In the tests of this wok 2.16 kg and 190 °C have been used as operative parameters). Since the MFR value is determined under fixed load conditions, it can be considered essentially as an extrusion rheometer and it represents a specific point on the shear stress versus shear rate curve, directly correlated to the viscosity of the melt [40]. Melt Volume Rate (MVR) of the polymer, instead, is defined as the volume (in cm^3) crossed by the melt acquired by the encoder that follows the movement of the piston during the test time. Melt flow rate (MFR) and melt volume rate (MVR) were recorded in 1 min, averaged over time, and expressed, respectively, in g/10 min and cm^3/10 min.

2.4. Mechanical tests

The mechanical characterisations were carried out, at room temperature, three days after the specimen's injection moulding. The specimens were stored in a dry keeper (SANPLATEC Corp., Osaka, Japan) at room temperature and 50% of humidity.

Tensile tests were carried out on the ISO 527-1A dog bone specimens by an MTS Criterion model 43 (MTS Systems Corporation, Eden Praire, MN, USA) universal tensile testing machine equipped with a 10 kN load cell and set with a cross head speed of 10 mm/min. During the tensile test a videoextensometer (Genie HM1024 Teledyne DALSA camera), interfaced with a computer running ProVis software (Fundamental Video Extensometer), recorded the axial and the transversal strain. The data in real time were transferred to MTS Elite software to collect both

Table 2
Main injection moulding parameters.

Main injection moulding parameters	PLA	PLA90_PCL10	PLA80_PCL20	PLA60_PBSA40
Temperature profile (°C)	180/180/185/185			
Mould temperature (°C)	60	60	55	50
Injection holding time (s)	5			
Cooling time (s)	30	30	35	35
Injection pressure (bar)	90	85	72	62

axial and transversal strains useful for the determination of the volume strain variation according to Eq. (1) [15].

$$\frac{\Delta V}{V_0} = (1+\varepsilon_1)(1+\varepsilon_2)^2 - 1 \quad (1)$$

Where $\Delta V/V_0$ is the volume variation, ε_1 is the longitudinal strain and ε_2 is the transversal strain. At least five specimens were tested for each composition. To be able to apply Eq. (1), dilatometry testes were carried out until the deformation of the specimens remained homogeneous (no presence of necking) [15].

Charpy impact test were carried out on a CEAST 9050 (INSTRON, Canton, MA, USA) apparatus according to ISO 179 test with parallelepiped specimens V-notched at 2 mm; at least eight specimens for each composition were tested and the mean value was reported.

J_{Ilim} is the fracture energy at the starting point of the crack propagation and it was calculated, with the above-mentioned MTS in three-point bending configuration, following the ESIS TC4 load separation protocol [39,41]; Single Edge Notched Bending (SENB) specimen having dimensions of 80 mm × 10 mm x 4 mm were tested at 1 mm/min in Three Points Bending (3 PB) configuration at 1 mm/min. The specimens adopted were cut in the middle in two different ways: "sharp" (half notched samples having 5 mm length) and "blunt" (punctured in the centre with a 2 mm diameter hole and then cut for half width). For the sharp specimens, compressed air was used to avoid the "notch closing" phenomenon caused by excessive overheating generated by the cutter; moreover a "sacrificial specimen" placed under the "good one" was used to guarantee a correct notch of the sample avoid plastic deformation around it. At least five specimens were tested for each composition. The J_{lim} was calculated following the Load Separation Criterion procedure [42,43]. Consequently, the load (P) vs. displacement (u) curve of sharp and blunt specimens was recorded (in the sharp specimens the fracture can propagate, while in the blunt specimens the crack cannot grow). Hence the variation of the load separation parameter (S_{sb}) was calculated according to Eq. (2):

$$S_{sb} = \frac{P_s}{P_b}\Big|_{u_{pl}} \quad (2)$$

the subscripts s and b indicate the sharp and the blunt notched specimens, respectively. The plastic displacement, u_{pl}, was calculated as follows (Eq. (3)):

$$u_{pl} = u - PC_0 \quad (3)$$

u is the total displacement and C_0 is the initial elastic specimen compliance. It must be kept in mind that for the polymers used (and more in general for ductile polymers), fracture initiation is a gradual complex process, characterized by the slow development of the crack front across the thickness of fracture transition [18,43,44]. This limit point is the pseudo-initiation of fracture and once that limit point was defined, the corresponding J_{lim} can be calculated by Eq. (4):

$$J_{lim} = \frac{2U_{lim}}{b(w-a_0)} \quad (4)$$

U_{lim} is the elastic behaviour limit point, b is the sample thickness, w is the sample width and a_0 is the initial crack length.

To detect graphically the point in which the crack propagation occurs, the 3 PB tests were carried out with the help of the previously mentioned Genie HM1024 Teledyne DALSA camera collecting photos every 20 s.

2.5. Optical analysis

The morphology of the injection moulded specimens was investigated by scanning electron microscope (SEM) (Quanta 450 FEG, Thermo Fisher Scientific, Waltham, MA, USA) on samples cryofractured in liquid nitrogen. SEM micrographs (at 4000X) of the PLA/PCL blends with different PCL amount were obtained. To better understand the micromechanical deformation processes detected during the dilatometry tests, the fracture surface of the tensile specimens used for dilatometric tests were investigated. Firstly, the specimen were cut in liquid nitrogen in their midsection; subsequently the broken specimen were cut again in liquid nitrogen along the tensile direction with a cutting plier. In this way, it was possible to observe the fracture surface of the specimen along its thickness and with direction parallel to the tensile direction. A schematization of the procedure adopted is reported in Fig. 1.

To avoid the build up of the charge, all the sample surfaces were sputtered (with a LEICA EM ACE 600 High Vacuum Sputter Coater, Wetzlar, Germany) with a thin layer of platinum.

3. Results and discussion

3.1. Main characterisation results

The MFR data, reported in Table 3, show an increment of MFR with the PCL content. PCL has a lower viscosity than PLA as demonstrated by its MFR value that is about ten times greater than that of PLA. As described in section 2.3 MFR can be defined as a "punctual viscosity" and this great MFR variation is also a difference in viscosity that can be mainly ascribed to the great difference in the melting temperature between PLA (that is around 150 °C) and PCL (that is around 60 °C) [40]. This marked disparity in viscosity between PLA and PCL significantly affects the blends viscosity and their processability. The MFR increment caused by the PCL addition, caused a decrement of the extruder head pressure that passed from 24 bar for PLA to 14 bar for PLA60_PCL40.

Also, the injection moulding process was affected by this viscosity change; although it was tried to keep the process parameters unchanged as possible, to obtain injection moulded specimens without imperfections some changes were done. In spite of the temperature profile was the same for all blends, an increment of the cooling time was necessary increasing the PCL amount. Moreover, a decrement of the mould temperature and injection pressure was necessary to counterbalance the viscosity decrement caused by the PCL increment.

The results of the tensile tests, summarized in Table 4, show how the main mechanical properties vary passing from neat PLA to pure PCL.

PLA is a brittle material with high stiffness and tensile strength but low elongation at break. Neat PLA fails without yielding. On the other hand, PCL is a ductile polymer with an elastic modulus more akin to an elastomer [22]. Consequently, as it could be expected and coherently with literature [27,30], the PCL addition reduces the PLA elastic modulus and stress at break while it slightly increases its elongation at break. Noteworthy is the Charpy impact resistance improvement; C.I.S. increases almost proportionally with the PCL content. From the mechanical results emerge some differences about the PCL toughening effect. In fact, with the addition of PCL, the tensile toughness increases slightly, while the impact resistance grows appreciably. Similar discrepancies between tensile toughness and impact strength data have been found in literature in other binary blends [10,18,45] and they were attributed to dissimilar deformation mechanisms that occurs when the loading conditions changes. In fact, tensile and impact tests are completely different being Charpy impact tests like a 3 PB test carried out at high-speed rate.

From the SEM micrographs reported in Fig. 2, it can be observed that the blends show a biphasic morphology that confirms the well-known immiscibility of PLA with PCL [46].

The interfacial adhesion for PLA/PCL blends, according to literature [46], is equal to 1.55 mN m^{-1}. The minor phase (PCL) is distributed in spherical droplets embedded into the PLA matrix. The droplets sizes increase with the PCL content consistently to what was already observed in literature [20,47] and this phenomenon is mainly ascribed to the increasing PCL amount that boosts the probability of PCL droplets to coalesce giving larger drop ellipsoidal size. For PLA60_PCL 40 the PCL amount is very high and the spherical PCL droplets become ellipsoidal

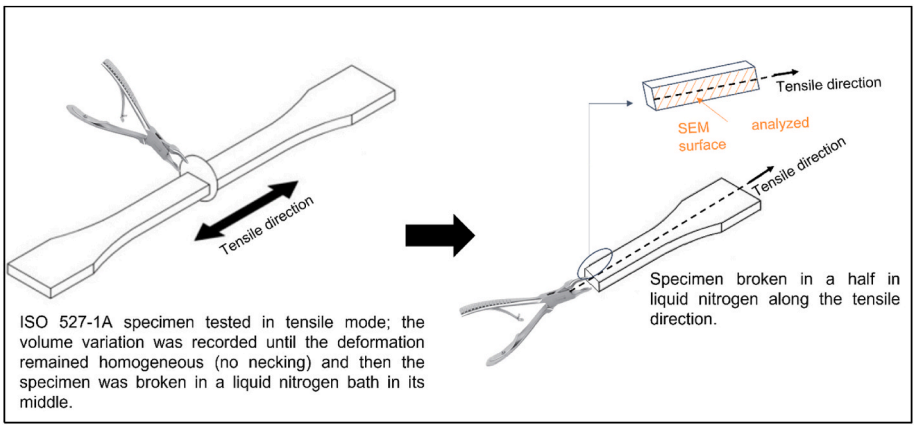

Fig. 1. Schematization of the procedure adopted to observe by SEM the micromechanical deformation process occurring during tensile test.

Table 3
MFR values.

Blend name	MFR (g/10 min)	MVR (g/10 min)
PLA	2.3 ± 0.3	1.8 ± 0.3
PLA90_PCL10	3.1 ± 0.5	2.4 ± 0.4
PLA80_PCL20	4.0 ± 0.7	3.2 ± 0.6
PLA60_PCL40	9.6 ± 2.6	8.5 ± 2.3
PCL	24.9 ± 1.6	25.8 ± 1.8

similarly to what was observed by Wu et al. [24], the orientation of these elliptic domains is influenced by the directionality of the molten material when it is injection moulded.

3.2. Micromechanical analysis and fracture mechanics results

The dilatational behaviour that a material undergoes to an applied stress (for example during tensile tests) can lead to an appreciated deformation mechanism in the bulk of the material; based on the *volume strain vs. strain* curve, it is possible to distinguish between: cavitational, dilational and deviatoric response [48].

The dilatometric curves obtained with the video-extensometer during the tensile tests, are reported in Fig. 3 where the volume strain (calculated with Eq. (1)) is reported as function of axial elongation. The dilatometric tests were carried out until the deformation of the specimens remained homogeneous.

Two different responses can be distinguished: a deviatoric response for PLA60_PCL40 and a cavitational response for PLA80_PCL20. For all blends the dilatometric curves, at the early stages of the deformation, behave in a similar manner with the volume strain that increases almost linearly with the deformation; then a change in the slope and shape of the curves, usually associated to a significant volume increment, is registered. The point in which this slope change occurs, can be interpreted as a deformation initiation value which prompts a certain micromechanical deformation process [15,28].

For the dilatometric curves that display cavitational response (like PLA80_PCL20), the intersection point at which the slope of the volume strain changes, corresponds the point in which the particle cavitation (or debonding) occurs. This process is followed by a second micromechanical deformation mechanism that is the growth of the generated voids along the tensile direction. The latter mechanism absorbs more energy respect to the particles cavitation stage [10]; thus it is the mechanicians main responsible of the enhanced elongation at break (reflected in enhanced tensile toughness). For materials having cavitational response, the cavitation type mechanism can produce voids that grow along tensile direction and then coalesce bringing to the final breakage of the material [15]. However, depending on the number of cavitated particles, on the particles/matrix interaction, on particles size and distributions, only cavitation mechanism can occur that leads to a smaller volume strain increment and to a reduced tensile toughness. Deeply analysing the dilatometric curves obtained for PLA90_PCL10 and PLA80_PCL20 it can be observed that, meanwhile the first part was almost the same, only PLA80_PCL20 formulation showed the change in the slope of the volume strain followed by its marked increment. Consequently, it can be deducted that only for PLA80_PCL20 the second micromechanical deformation mechanism occurred that it is responsible of the better elongation at break improvement. On the other hand, for PLA90_PCL10 presumably only particles cavitation occurred.

For PLA60_PCL40, the dilatometric curve is different and has a deviatoric response. Generally, when this type of response appears, the volume strain increases almost linearly with the stress until the stress reached by the material will cause its deformation that will change the shape of the material, but it will not change its volume [48]. Materials in which shear yielding [49] occurs will lead to a constant value of the volume strain with deformation leading to a deviatoric response. However, the presence of deviatoric response does not mean necessarily that only shear yielding of the matrix occurs; in fact, even if this mechanism can be considered predominant (due to the different shape of the deviatoric response respect to cavitation ones), it has been observed in literature that both cavitation and shear yielding can occur [48].

In Fig. 4 are summarized the typical micromechanical deformation mechanisms occurred in the PLA/PCL blends at which are associated different zones and shapes of the resulting volumetric strain curves (as

Table 4
Main mechanical properties obtained from tensile and impact tests.

Blend name	Elastic Modulus (GPa)	Stress at break (MPa)	Elongation at break (MPa)	Stress at yield (MPa)	Elongation at yield (%)	Charpy impact strength (C.I.S.)
PLA	3.5 ± 0.1	62.7 ± 1.7	3.7 ± 0.3	No yield	No yield	2.8 ± 0.3
PLA90_PCL10	3.0 ± 0.1	24.2 ± 1.2	18.9 ± 6.9	57 ± 0.5	1.6 ± 0.1	3.9 ± 0.4
PLA80_PCL20	2.9 ± 0.1	21.8 ± 1.3	24.9 ± 3.3	47.5 ± 1.7	1.9 ± 0.1	5.5 ± 0.3
PLA60_PCL40	1.5 ± 0.1	18.2 ± 1.9	42.4 ± 3.2	34.8 ± 0.7	3.9 ± 0.1	8.4 ± 0.4
PCL	0.4 ± 0.1	Not broken	>500%	16.5 ± 0.1	19.9 ± 0.1	11.9 ± 0.4

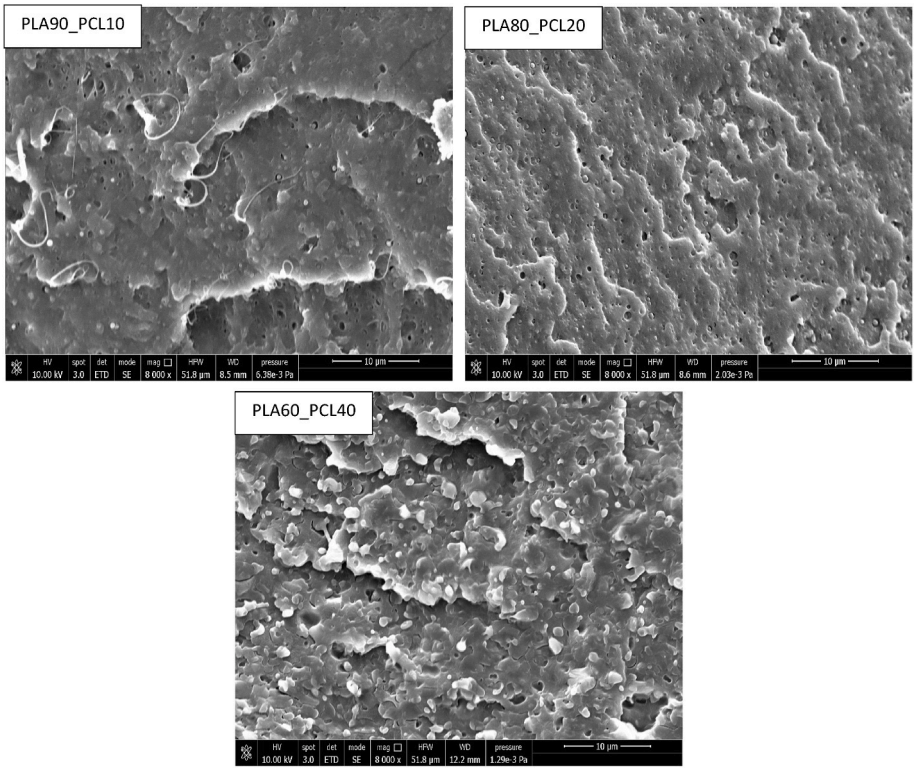

Fig. 2. SEM images at 8000X of PLA/PCL binary blends.

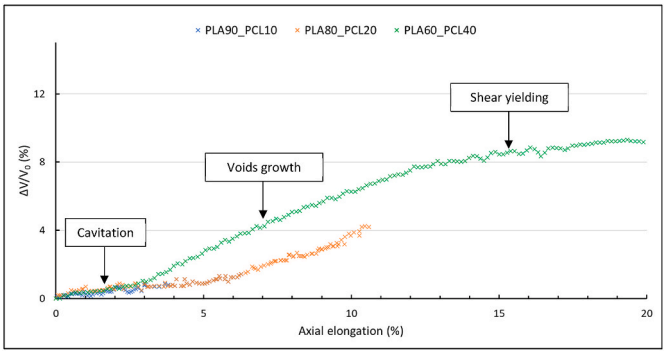

Fig. 3. Volume strain–strain curves of PLA-PCL binary blends.

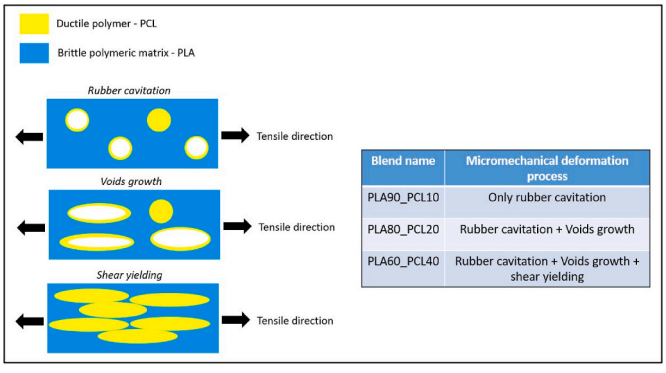

Blend name	Micromechanical deformation process
PLA90_PCL10	Only rubber cavitation
PLA80_PCL20	Rubber cavitation + Voids growth
PLA60_PCL40	Rubber cavitation + Voids growth + shear yielding

Fig. 4. Sketch of the micromechanical deformation mechanisms occurring in PLA/PCL blends.

reported in Fig. 3).

For all systems analysed, the micromechanical deformation mechanism must be confirmed by SEM analysis, reported in Fig. 5, of the specimens cryofractured along the tensile direction according the procedure schematized in Fig. 1. For PLA90_PCL10, in accordance with the volume strain data, the binary blend shows only the cavitation of the PCL particles from the PLA matrix. In this stage, the interfacial adhesion plays an important role: a high adhesion leads to the internal cavitation of the rubber particles (the voids are generated within the rubber particles), while low adhesion leads to the detachment of the rubber particles from the matrix (debonding) [50,51]. The number of cavitated particles for PLA90_PCL10 is not a high amount and no voids growth mechanism along the draw direction was observed in accordance with the little strain volume registered and the poor increment of the tensile toughness. However, the areas in which the cavitation mechanism occurred are easily distinguishable; the cavitated PCL particles are localised along clearly identifiable dilatational bands (dashed yellow lines) developed almost perpendicularly to the draw direction. The formation of these dilatational bands is typical of rubber toughened systems and has been found in literature for PLA/PBAT [29], Nylon/ABS [52], poly(styrene-co-acrylonitrile) (PSAN) and acrylonitrile–butadiene–styrene (ABS) [53] binary blends. The dilatational bands form a planar array of debonded particles where the matrix around the voids undergoes to higher shear strains and reduced constraints on the plastic flow [54].

For PLA80_PCL20, it can be observed that not only cavitation occurred; in accordance with the dilatometric curves, also the voids growth along the tensile direction happened. The latter mechanism is mainly responsible of the better elongation at break and of the marked volume strain increment. It must be pointed out that the two micromechanical deformation mechanisms are competitive and the way in which one prevails on the other depends on the matrix properties and by the local stress distribution; only when the volume strain energy is greater than that required for the creation of the void surface area the voids growth occurs [53]. The formation of the dilatational bands is

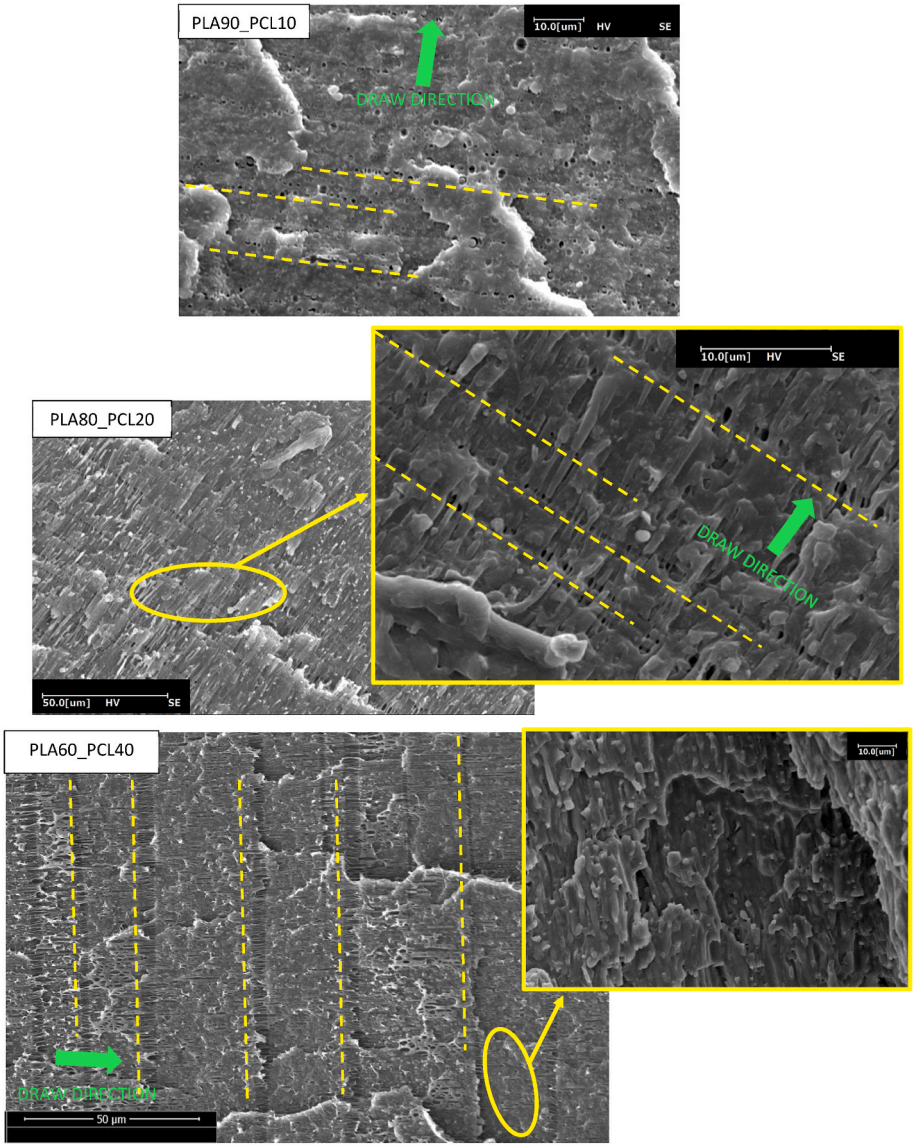

Fig. 5. SEM micrographs of the cryo-fractured surface of tensile PLA/PCL specimens along the draw direction.

clearer visible for PLA80_PCL20 in which it is highlighted how the deboning of the PCL particles and the voids growth along the tensile direction is localised within the dilatational bands.

The SEM micrograph of PLA60_PCL40 helps to better clarify the dilatometric results. Even if the shape of the dilatometric curve suggested the presence of shear yielding, it can be noticed that three concurrent micromechanical deformation processes occurred. One is the shear yielding (highlighted in the zoom window) that is predominant and it is responsible of the deviatoric response. However, also cavitation, followed by the voids growth occurred localized in the dilatational bands that in this case are markedly visible and present in higher amount than in PLA80_PCL20 blend. The higher number of dilatational bands and the higher extension of the voids growth coupled with the prevalence of the shear yielding are responsible of the marked increment of the elongation at break. Furthermore, the higher presence of zones in which shear yielding occurred means that the material will continue to deform under stress by changing shape but not its volume leading to a shear yielding as the main failure mechanism [15]. Also, the fracture behaviour of PLA/PCL is dissimilar and strongly dependant on the PCL content.

Moreover, it was observed that the binary blends behave differently to pure polymers. Fig. 6 shows some significant load-deflection curves (from 3 PB tests at 1 mm/min) of the studied blends and pure polymers correlated with frames corresponding to well-defined points on the curves. The brittle behaviour of PLA is evident; this material can absorb a high amount of energy before the crack initiation (withstanding up to 125 N); once that the initiation occurs, the crack propagates instantaneously causing catastrophic failure and low evidence of plastic deformation.

As the amount of PCL into the PLA increases, the curves show a decrement of the crack initiation load coherently to what observed in literature [55]; nevertheless, the crack progress is progressively more hindered and slowed down with a considerable increase in plastic deformation and, therefore, in specimen whitening. PCL, which has a low T_g (−60 °C [55]), behaves like a rubber at room temperature by toughening the PLA matrix and preventing instantaneous crack propagation [47]. This last statement is evident in the behaviour of pure PCL where, after 3.5 mm of crosshead displacement, there is no maximum reached in the curve, the pre-crack of the specimen is widening and the blunting of the crack apex is almost complete, thus preventing the formation of a tensional state conducive to crack propagation.

For ductile materials the energy absorbed at the start of the crack propagation was investigated through a protocol based on the "load separation criterion", as expressed in section 2.4. This criterion is not

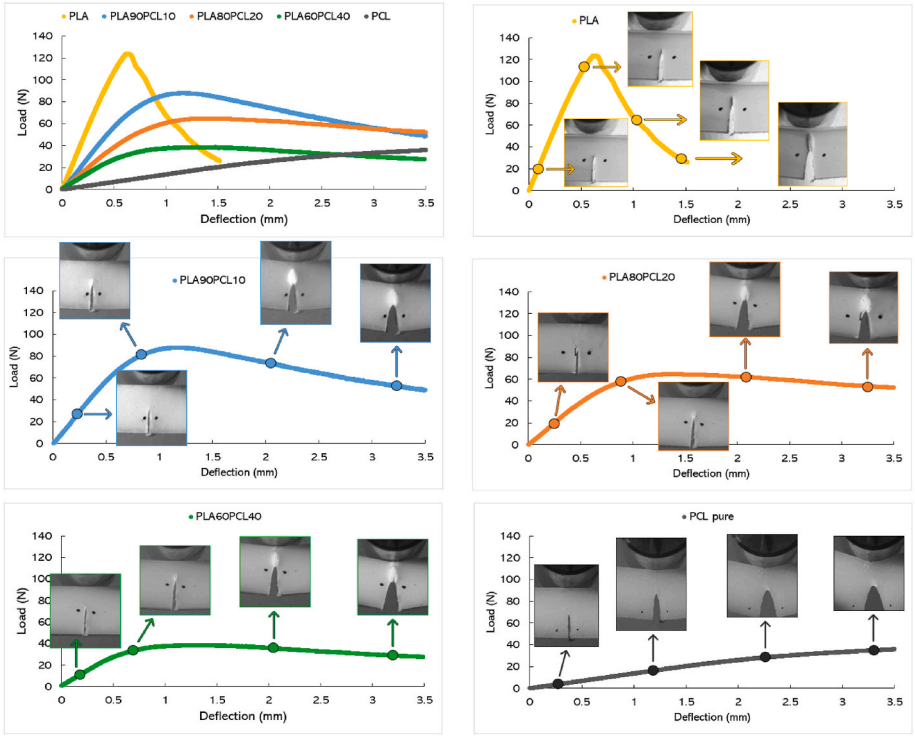

Fig. 6. Results of three-point bending tests showing load-deflection curves and fracture propagation through in-live micrographs.

applicable to brittle materials or elastomers [56] therefore, the comparison was only made on the PLA/PCL blends. The results obtained with these "slow rate" tests (Fig. 7) can be compared with impact tests (Table 4) highlighting an important difference.

The energy stored prior to crack propagation is higher for the material with the larger amount of PCL, however the difference is not so marked between the formulations because the toughening activity occurs along the entire section and not only at the crack apex [57]. This advancement speed becomes gradually slower as the PCL content increases. An evident confirmation of this statement can be evaluated by making a comparison with the Charpy Impact strength data of Table 4 in which all the energy necessary for the failure of the specimen is contained (both crack initiation and crack propagation energies). Van der Wal et al. [58] demonstrated that the energy accumulated by the specimen during the crack propagation increases with the rubber content; in particular, the speed at which the blend become brittle will be progressively higher increasing the rubber amount. In a previous work Gigante et al. [18], instead, demonstrated that test speed influenced the crack initiation energy in PLA-PBAT blends and the glass transition temperature of the PBAT dispersed phase was not so low to guarantee a toughness increment at impact speed because the sum of crack initiation and propagation energy were lower than stored energy before the crack initiation evaluated at lower speeds. In this work, instead, PCL can guarantee a toughness improvement even at impact speeds moving the materials towards higher Charpy impact strength values, thanks to its very low glass transition temperature (−60 °C).

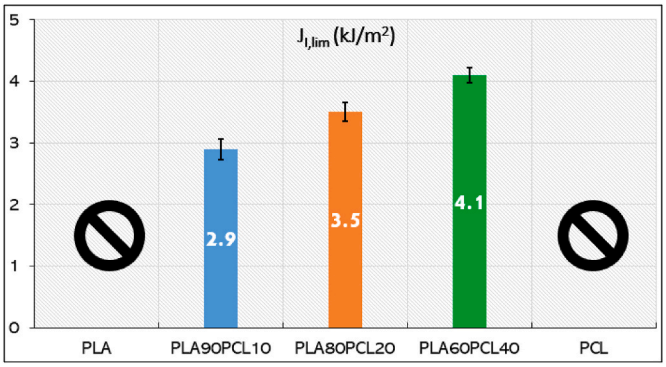

Fig. 7. Results of $J_{I,lim}$ for PLA-PCL blends.

4. Conclusions

In this work dilatometric studies to investigate the micromechanical deformation processes and fracture mechanics of PLA/PCL blends containing different PCL amount (at 10, 20 and 40 wt%) were investigated. Thanks to SEM analysis, the formation of dilational bands was observed, oriented perpendicularly to the draw direction, from which the cavitation of PCL particles started. Coupling SEM analysis with the dilatometric curves it was possible to distinguish different micromechanical deformation process, some of them were competitive and occurred simultaneously. For the blend containing 10 wt% of PCL only the cavitation of a small portion of PCL particles occurred and this was reflected in the low ductility increment. When 20 wt% of PCL was added both cavitation and the voids growth along the tensile direction was observed that generated an increment not only of the volume strain but also of the elongation at break. Finally, for the blend containing 40 wt% of PCL, apart from cavitation and voids growth, it was observed that the predominating micromechanical deformation process was the shear yielding (that provoked a deviatoric response of the dilatometric curve); the presence of these three mechanisms increased further the final elongation at break of the material.

The fracture response of PLA/PCL blends in a high-speed test (Charpy impact test) and a low-speed test (J_{lim} corresponding to the energy absorbed by the material when the crack starts to propagate) showed that increasing the PCL content the fracture resistance of the material increases thanks to the major content of PCL that has a rubbery behaviour.

Funding

This research was funded by the Bio-Based Industries Joint Undertaking under the European Union Horizon 2020 research program (BBI-H2020), BIONTOP project, grant number G.A 837761.

Author statement

Conceptualization: Laura Aliotta, Vito Gigante, Andrea Lazzeri.
Data curation: Laura Aliotta, Vito Gigante, Maria-Beatrice Coltelli, Funding **acquisition and resources:** Maria-Beatrice Coltelli.
Investigation: Laura Aliotta, Vito Gigante.
Methodology: Laura Aliotta, Vito Gigante.
Visualization: Laura Aliotta, Vito Gigante, Maria-Beatrice Coltelli, Ruben Geerinck.
Supervision: Andrea Lazzeri.
Validation: Andrea Lazzeri, Maria-Beatrice Coltelli.
Writing - original draft: Laura Aliotta, Vito Gigante,
Writing - review & editing: Andrea Lazzeri, Maria-Beatrice Coltelli, Ruben Geerinck.

Declaration of competing interest

The authors declare that they have no known competing financial interests or personal relationships that could have appeared to influence the work reported in this paper.

Data availability

Data will be made available on request.

Acknowledgments

This research was partly funded by the Bio-Based Industries Joint Undertaking under the European Union Horizon 2020 Research Program (BBI-H2020), BIONTOP project, Grant Number G.A. 837761. The authors acknowledge Ingevity for cooperation in providing the PCL CAPA6500.

References

[1] F.P. la Mantia, M. Morreale, L. Botta, M.C. Mistretta, M. Ceraulo, R. Scaffaro, Degradation of polymer blends: a brief review, Polym. Degrad. Stabil. 145 (2017) 79–92, https://doi.org/10.1016/j.polymdegradstab.2017.07.011.
[2] V. Mittal, T. Akhtar, N. Matsko, Mechanical, thermal, rheological and morphological properties of binary and ternary blends of PLA, TPS and PCL, Macromol. Mater. Eng. 300 (2015) 423–435, https://doi.org/10.1002/mame.201400332.
[3] G.E. Luckachan, C.K.S. Pillai, Biodegradable polymers- A review on recent trends and emerging perspectives, J. Polym. Environ. 19 (2011) 637–676, https://doi.org/10.1007/s10924-011-0317-1.
[4] T.D. Moshood, G. Nawanir, F. Mahmud, F. Mohamad, M.H. Ahmad, A.A. Ghani, Expanding policy for biodegradable plastic products and market dynamics of bio-based plastics: challenges and opportunities, Sustainability (2021) 13, https://doi.org/10.3390/su13116170.
[5] R. Auras, B. Harte, S. Selke, An overview of polylactides as packaging materials, Macromol. Biosci. 4 (2004) 835–864, https://doi.org/10.1002/mabi.200400043.
[6] I.S.M.A. Tawakkal, M.J. Cran, J. Miltz, S.W. Bigger, A review of poly(lactic acid)-based materials for antimicrobial packaging, J. Food Sci. 79 (2014), https://doi.org/10.1111/1750-3841.12534.
[7] N. Sundar, P. Keerthana, S.A. Kumar, G.A. Kumar, S. Ghosh, Dual purpose, bio-based polylactic acid (PLA)-polycaprolactone (PCL) blends for coated abrasive and packaging industrial coating applications, J. Polym. Res. 27 (2020), https://doi.org/10.1007/s10965-020-02320-0.
[8] I. Lukic, J. Vulic, J. Ivanovic, Antioxidant activity of PLA/PCL films loaded with thymol and/or carvacrol using scCO2 for active food packaging, Food Packag. Shelf Life 26 (2020), https://doi.org/10.1016/j.fpsl.2020.100578.
[9] S. Krishnan, P. Pandey, S. Mohanty, S.K. Nayak, Toughening of polylactic acid: an overview of research progress, Polym. Plast. Technol. Eng. 55 (2016) 1623–1652, https://doi.org/10.1080/03602559.2015.1098698.
[10] L. Aliotta, V. Gigante, O. Acucella, F. Signori, A. Lazzeri, Thermal , mechanical and micromechanical analysis of PLA/PBAT/POE-g-GMA extruded ternary blends, Front. Mater. 7 (2020) 1–14, https://doi.org/10.3389/fmats.2020.00130.
[11] S. Su, R. Kopitzky, S. Tolga, S. Kabasci, Polylactide (PLA) and its blends with poly (butylene succinate)(PBS): a brief review, Polymers 11 (2019) 1193.
[12] A. Bhatia, R.K. Gupta, S.N. Bhattacharya, H.J. Choi, Compatibility of biodegradable poly (lactic acid) (PLA) and poly (butylene succinate) (PBS) blends for packaging application, Korea Australia Rheology, Journal 19 (2007) 125–131, https://doi.org/10.1155/2010/287082.
[13] M. Nofar, R. Salehiyan, U. Ciftci, A. Jalali, A. Durmuş, Ductility improvements of PLA-based binary and ternary blends with controlled morphology using PBAT, PBSA, and nanoclay, Compos. B Eng. 182 (2020), https://doi.org/10.1016/j.compositesb.2019.107661.
[14] X. Zhao, D. Zhang, S. Yu, H. Zhou, S. Peng, Recent advances in compatibility and toughness of poly(lactic acid)/poly(butylene succinate) blends, E-Polymers 21 (2021) 793–810, https://doi.org/10.1515/epoly-2021-0072.
[15] L. Aliotta, A. Vannozzi, I. Canesi, P. Cinelli, M.-B. Coltelli, A. Lazzeri, Poly(Lactic acid) (PLA)/poly(butylene succinate-co-adipate) (PBSA) compatibilized binary biobased blends: melt fluidity, morphological, thermo-mechanical and micromechanical analysis, Polymers 13 (2021), https://doi.org/10.3390/polym13020218.
[16] L. Aliotta, A. Vannozzi, P. Cinelli, M. Coltelli, A. Lazzeri, Essential work of fracture and evaluation of the interfacial adhesion of plasticized PLA/PBSA blends with the addition of wheat bran by-product, Polymers 14 (2022) 1–19, https://doi.org/10.3390/polym14030615.
[17] M. Nofar, A. Tabatabaei, H. Sojoudiasli, C.B. Park, P.J. Carreau, M.-C. Heuzey, M. R. Kamal, Mechanical and bead foaming behavior of PLA-PBAT and PLA-PBSA blends with different morphologies, Eur. Polym. J. 90 (2017) 231–244, https://doi.org/10.1016/j.eurpolymj.2017.03.031.
[18] V. Gigante, I. Canesi, P. Cinelli, M.B. Coltelli, A. Lazzeri, Rubber toughening of polylactic acid (PLA) with poly(butylene adipate-co-terephthalate) (PBAT): mechanical properties, fracture mechanics and analysis of ductile-to-brittle behavior while varying temperature and test speed, Eur. Polym. J. 115 (2019) 125–137, https://doi.org/10.1016/j.eurpolymj.2019.03.015.
[19] X. Zhao, H. Hu, X. Wang, X. Yu, W. Zhou, S. Peng, Super tough poly(lactic acid) blends: a comprehensive review, RSC Adv. 10 (2020) 13316–13368, https://doi.org/10.1039/d0ra01801e.
[20] I. Fortelny, A. Ujcic, L. Fambri, M. Slouf, Phase structure, compatibility, and toughness of PLA/PCL blends: a review, Front. Mater. 6 (2019), https://doi.org/10.3389/fmats.2019.00206.
[21] A.K. Matta, R.U. Rao, K.N.S. Suman, V. Rambabu, Preparation and characterization of biodegradable PLA/PCL polymeric blends, Procedia Mater. Sci. 6 (2014) 1266–1270, https://doi.org/10.1016/j.mspro.2014.07.201.
[22] C.L. Simões, J.C. Viana, A.M. Cunha, Mechanical properties of poly(ε-caprolactone) and poly(lactic acid) blends, J. Appl. Polym. Sci. 112 (2009) 345–352, https://doi.org/10.1002/app.29425.
[23] Y. Zhang, D. Wu, M. Zhang, W. Zhou, C. Xu, Effect of steady shear on the morphology of biodegradable poly(ε-caprolactone)/polylactide blend, Polym. Eng. Sci. 49 (2009) 2293–2300, https://doi.org/10.1002/pen.21456.
[24] D. Wu, Y. Zhang, M. Zhang, W. Zhou, Phase behavior and its viscoelastic response of polylactide/poly(ε-caprolactone) blend, Eur. Polym. J. 44 (2008) 2171–2183, https://doi.org/10.1016/j.eurpolymj.2008.04.023.
[25] I. Moura, A.v. Machado, F.M. Duarte, R. Nogueira, Biodegradability assessment of aliphatic polyesters-based blends using standard methods, J. Appl. Polym. Sci. 119 (2011) 3338–3346, https://doi.org/10.1002/app.32966.
[26] V. Thaore, D. Chadwick, N. Shah, Sustainable production of chemical intermediates for nylon manufacture: a techno-economic analysis for renewable production of caprolactone, Chem. Eng. Res. Des. 135 (2018) 140–152, https://doi.org/10.1016/J.CHERD.2018.05.026.
[27] I. Navarro-Baena, V. Sessini, F. Dominici, L. Torre, J.M. Kenny, L. Peponi, Design of biodegradable blends based on PLA and PCL: from morphological, thermal and mechanical studies to shape memory behavior, Polym. Degrad. Stabil. 132 (2016) 97–108, https://doi.org/10.1016/j.polymdegradstab.2016.03.037.
[28] B. Pukánszky, M. van Es, F.H.J. Maurer, G. Vörös, Micromechanical deformations in particulate filled thermoplastics: volume strain measurements, J. Mater. Sci. 29 (1994) 2350–2358, https://doi.org/10.1007/BF00363426.
[29] V. Gigante, L. Bosi, P. Parlanti, M. Gemmi, L. Aliotta, A. Lazzeri, Analysis of the damage mechanism around the crack tip for two rubber-toughened PLA-based blends, Polymers 13 (2021) 4053, https://doi.org/10.3390/polym13224053.
[30] C.-C. Chen, J.-Y. Chueh, H. Tseng, H.-M. Huang, S.-Y. Lee, Preparation and characterization of biodegradable PLA polymeric blends, Biomaterials 24 (2003) 1167–1173, https://doi.org/10.1016/S0142-9612(02)00466-0.
[31] M. Todo, T. Takayama, Fracture Mechanisms of Biodegradable PLA and PLA/PCL Blends, Biomaterials-Physics and Chemistry, 2011.
[32] A. Ostafinska, I. Fortelný, J. Hodan, S. Krejčíková, M. Nevoralová, J. Kredatusová, Z. Kruliš, J. Kotek, M. Šlouf, Strong synergistic effects in PLA/PCL blends: impact of PLA matrix viscosity, J. Mech. Behav. Biomed. Mater. 69 (2017) 229–241.
[33] S. Wachirahuttapong, C. Thongpin, N. Sombatsompop, Effect of PCL and compatibility contents on the morphology, crystallization and mechanical properties of PLA/PCL blends, Energy Proc. 89 (2016) 198–206, https://doi.org/10.1016/j.egypro.2016.05.026.
[34] S. Wachirahuttapong, C. Thongpin, N. Sombatsompop, Effect of PCL and compatibility contents on the morphology, crystallization and mechanical properties of PLA/PCL blends, in: Energy Procedia, Elsevier Ltd, 2016, pp. 198–206, https://doi.org/10.1016/j.egypro.2016.05.026.
[35] Z. Bartczak, A. Argon, R. Cohen, M. Weinberg, Toughness mechanism in semi-crystalline polymer blends - I. HDPE toughened with rubber, Polymer (Guildf) 40 (1999) 2331–2346. http://www.sciencedirect.com/science/article/pii/S0032386198004455.

[36] C. G'sell, J.M. Hiver, A. Dahoun, A. Souahi, Video-controlled Tensile Testing of Polymers and Metals beyond the Necking Point, 1992.
[37] F. Rezgui, M. Swistek, J.M. Hiver, C. G'Sell, T. Sadoun, Deformation and damage upon stretching of degradable polymers (PLA and PCL), Polymer (Guildf) 46 (2005) 7370–7385, https://doi.org/10.1016/j.polymer.2005.03.116.
[38] F. Baldi, S. Agnelli, T. Riccò, On the determination of the point of fracture initiation by the load separation criterion in J-testing of ductile polymers. https://doi.org/10.1016/j.polymertesting.2013.08.007, 2013.
[39] F. Baldi, S. Agnelli, T. Riccò, On the applicability of the load separation criterion in determining the fracture resistance (JIC) of ductile polymers at low and high loading rates. https://doi.org/10.1007/s10704-010-9510-9, 2010.
[40] A.S. Luyt, S. Gasmi, Influence of blending and blend morphology on the thermal properties and crystallization behaviour of PLA and PCL in PLA/PCL blends, J. Mater. Sci. 51 (2016) 4670–4681, https://doi.org/10.1007/s10853-016-9784-z.
[41] C.R. Bernal, P.E. Montemartini, P.M. Frontini, The use of load separation criterion and normalization method in ductile fracture characterization of thermoplastic polymers, J. Polym. Sci. B Polym. Phys. 34 (1996) 1869–1880, https://doi.org/10.1002/(SICI)1099-0488 (199608)34:11<1869::AID-POLB4>3.0.CO;2-N.
[42] M.H. Sharobeam, J.D. Landes, The load separation criterion and methodology in ductile fracture mechanics, Int. J. Fract. 47 (1991) 81–104, https://doi.org/10.1007/BF00032571.
[43] S. Agnelli, F. Baldi, A Testing Protocol for the Construction of the "Load Separation Parameter Curve" for Plastics, 2013.
[44] S. Agnelli, F. Baldi, T. Riccò, A tentative application of the energy separation principle to the determination of the fracture resistance (JIc) of rubbers. https://doi.org/10.1016/j.engfracmech.2012.04.020, 2012.
[45] K. Zhang, V. Nagarajan, M. Misra, A.K. Mohanty, Supertoughened renewable PLA reactive multiphase blends system: phase morphology and performance, ACS Appl. Mater. Interfaces 6 (2014) 12436–12448.
[46] J. Urquijo, G. Guerrica-Echevarría, J.I. Eguiazábal, Melt processed PLA/PCL blends: effect of processing method on phase structure, morphology, and mechanical properties, J. Appl. Polym. Sci. 132 (2015), https://doi.org/10.1002/app.42641 n/a-n/a.
[47] A. Ostafinska, I. Fortelny, M. Nevoralova, J. Hodan, J. Kredatusova, M. Slouf, Synergistic effects in mechanical properties of PLA/PCL blends with optimized composition, processing, and morphology, RSC Adv. 5 (2015) 98971–98982, https://doi.org/10.1039/c5ra21178f.
[48] S.I. Naqui, I.M. Robinson, Tensile dilatometric studies of deformation in polymeric materials and their composites, J. Mater. Sci. 28 (1993) 1421–1429, https://doi.org/10.1007/BF00363333.
[49] M.E.J. Dekkers, D. Heikens, Crazing and shear deformation in glass bead-filled glassy polymers, J. Mater. Sci. 20 (1985) 3873–3880, https://doi.org/10.1007/BF00552375.
[50] R.A. Pearson, A.F. Yee, Toughening mechanisms in elastomer-modified epoxies - Part 3 the effect of cross-link density, J. Mater. Sci. 24 (1989) 2571–2580, https://doi.org/10.1007/BF01174528.
[51] L. Aliotta, V. Gigante, M.-B. Coltelli, A. Lazzeri, Volume change during creep and micromechanical deformation processes in PLA–PBSA binary blends, Polymers 13 (2021), https://doi.org/10.3390/polym13142379.
[52] A. Lazzeri, C.B. Bucknall, Dilatational bands in rubber-toughened polymers, J. Mater. Sci. 28 (1993) 6799–6808, https://doi.org/10.1007/BF00356433.
[53] C.B. Bucknall, D.S. Ayre, D.J. Dijkstra, Detection of rubber particle cavitation in toughened plastics using thermal contraction tests, Polymer (Guildf) 41 (2000) 5937–5947.
[54] A. Lazzeri, C.B. Bucknall, Recent Developments in the Modeling of Dilatational Yielding in Toughened Plastics, Toughening of Plastics: Advances in Modeling and Experiments, 2000, p. 264.
[55] I. Fortelny, A. Ujcic, L. Fambri, M. Slouf, Phase structure, compatibility, and toughness of PLA/PCL blends: a review, Front. Mater. 6 (2019), https://doi.org/10.3389/fmats.2019.00206.
[56] A. Gosch, F.J. Arbeiter, S. Agnelli, M. Berer, G. Pinter, F. Baldi, J-testing of polymers via the load separation criterion based ESIS TC4 procedure: effect of the specimen size, Polym. Test. 89 (2020), 106637, https://doi.org/10.1016/J.POLYMERTESTING.2020.106637.
[57] L.F. Gockowski, N.D. Dolinski, R. Chavez, N. Cohen, F. Eisenreich, S. Hecht, R. M. McMeeking, C.J. Hawker, M.T. Valentine, Engineering crack tortuosity in printed polymer–polymer composites through ordered pores, Mater. Horiz. 7 (2020) 1854–1860, https://doi.org/10.1039/D0MH00331J.
[58] A. van der Wal, R.J. Gaymans, Polypropylene–rubber blends: 3. The effect of the test speed on the fracture behaviour, Polymer (Guildf) 40 (1999) 6045–6055, https://doi.org/10.1016/S0032-3861(99)00214-1.